Transient Response Control of Two-Mass System via Polynomial Approach

Yue Qiao[a], **Junyi Cao**[c], **Chengbin Ma**[a,b,*]
[a] Univ. of Michigan-Shanghai Jiao Tong Univ. Joint Institute
[b] School of Mechanical Engineering
Shanghai Jiao Tong University
No. 800 Dongchuan Road, Shanghai 200240
[c] School of Mechanical Engineering
Xi'an Jiaotong University, Xi'an 710049
P. R. China
Email: chbma@sjtu.edu.cn

This paper discusses the application of polynomial method in the transient response control of a benchmark two-mass system. It is shown that transient responses can be directly addressed by specifying the so-called characteristic ratios and the generalized time constant. The nominal characteristic ratio assignment is a good starting point for controller design. And the characteristic ratios with lower indices have a more dominant influence. Two practical low-order control configurations, the IP (Integral-Proportional) and m-IPD (modified-Integral-Proportional-Derivative) controllers are designed. The primary design strategy of the controllers is to guarantee the lower-index characteristic ratios to be equal to their nominal values, while the higher-index characteristic ratios are determined by the interaction with the generalized time constant and the limits imposed by zeros, a specific control configuration, etc. The demonstrated relationship between the transient responses and the assignments of characteristic ratios and generalized time constant in simulation and experiments explains the effectiveness of the polynomial-method-based controller design.

1 Introduction

In most control problems, time response is the final evaluation of the performance of the control system. However, there is limited work done for control parameter design directly relating to the transient characteristics. It is a continuing interest in designing controllers that have clear physical meaning in the transient response of a closed-loop system. Besides the well-known classical and modern control theories, there is an alternative approach called algebraic design using polynomial expressions (i.e., polynomial method). In the method, the so-called characteristic ratios are reported to have a strong relationship with the damping (i.e., the overshoot) of a closed-loop system, while the speed of response relates to generalized time constant [1] [2]. Unlike the trial-and-error-based design techniques in classical control theory, the transient time response can be explicitly controlled by specifying the characteristic ratios and the generalized time constant. Naslin empirically observed these relationships in 1960s [3]. An important contribution is attributed to Manabe, who proposed the Coefficient Diagram Method (CDM) based on Naslin's findings and the Lipatov-Sokolov stability criterion [4]. Using the CDM method, he designed controllers for many successful industrial applications.

Since polynomial method uses the closed-loop characteristic polynomial, a generalized controller design and discussion are possible. In its design procedure, control configuration is defined at the beginning. The coefficients of the characteristic polynomial are then determined under a specific assignment of characteristic ratios and generalized time constant. Therefore, the polynomial method is suitable as a general approach to design low-order controllers. This characteristics is desirable for real industrial applications. In this paper, the transient response control of a classical benchmark two-mass system is discussed due to the generality of the control problem and the accessible experimental facility. Many electric drive systems in industry can be modeled as two-mass systems from traditional applications such as steel rolling mills and elevators to the latest ones in electric vehicles and wind turbines. The analysis of the two-mass system also gives a good starting point and fruitful results for dealing with more complex systems.

The benchmark two-mass control problem is challenging because only the velocity of the drive side is assumed measurable, whereas driving torque, load torque and the velocity of the load side are not measurable [5]. Various approaches have been proposed for the two-mass system control during the past decade. Generally speaking, the controller design of the two-mass system falls into a category of control problems treated by modern control theory that usually leads to complicated high-order controllers with difficul-

ties in weighting function selection, parameter tuning, etc. Meanwhile, the low-order PID controllers and their modifications are predominant in industry. Improvements on the design of low-order controllers using the polynomial method would be both theoretically and practically important.

This paper presents new results to directly control the transient response of a real torsion system via the polynomial approach [7]. The torsion system is modeled by a benchmark two-mass system, in which the tendency of pole/zero cancellation and limitations imposed by jω-axis zeros make the controller design difficult, especially when the ratio of drive inertia to total inertia (i.e. inertia ratio) is large. All-pole closed-loop systems are first used for a preliminary discussion on the adjustment of overshoot and the speed of response by specifying characteristic ratios and generalized time constant, respectively. Nominal characteristic ratio assignments (CRAs) are exactly determined for nonovershooting step responses. Then the design of two low-order controllers, IP (Integral-Proportional) and m-IPD (modified-Integral-Proportional-Derivative) controllers are discussed based on the assignment of characteristic ratios and their interactive relationship with the generalized time constant, while in Ref. [7], the two controllers are simply designed under the nominal CRAs, and thus fixed generalized time constants too. This improvement enables a better tradeoff between damping and robustness. Finally, all the theoretical analysis and controller design are confirmed experimentally using the laboratory torsion test bench.

2 Laboratory Torsion System

As shown in Fig. 1, the test bench is a torsion system that emulates a two-mass system. The drive torque is transmitted from drive servomotor to the shaft by gears with a gear ratio of 1:2. Under the condition of close-to-zero gear backlash, the torsion system is usually modeled as a well-known benchmark two-mass system as shown in Fig. 1(b), where K_s is the spring coefficient, while J_m and J_l are the inertias of the drive and load sides, respectively. It should be noticed that the internal damping of the shaft is sometimes also taken into consideration. The transfer function between driving torque T_m and angular velocity of the drive side ω_m can be derived as

$$P(s) = \frac{s^2 + \omega_a^2}{J_m s(s^2 + \omega_r^2)}, \tag{1}$$

where ω_r and ω_a are the resonance frequency and anti-resonance frequency,

$$\omega_r = \sqrt{K_s\left(\frac{1}{J_m} + \frac{1}{J_l}\right)} \text{ and } \omega_a = \sqrt{\frac{K_s}{J_l}}, \tag{2}$$

respectively.

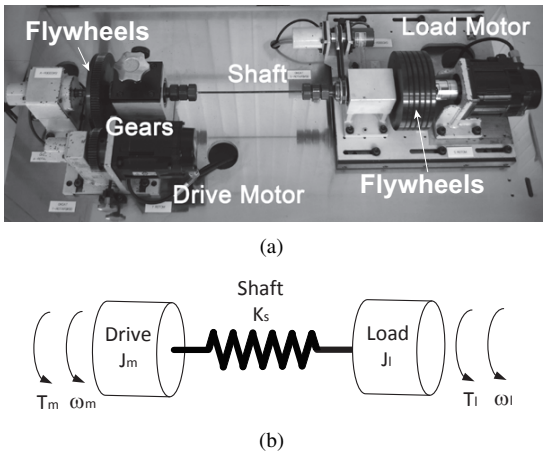

Fig. 1. The torsion test bench. (a) Experimental setup. (b) Two-mass model.

The model in Eqn. (1) can be further normalized as

$$P_n(s^*) = \frac{s^{*2} + 1}{qs^{*3} + s^*} \tag{3}$$

by replacing the Laplace operator s with $s^*=s/\omega_a$. Here q is the so-called inertia ratio defined as

$$q = \frac{J_m}{J_m + J_l}. \tag{4}$$

The normalized resonance frequency and anti-resonance frequency are then

$$\omega_r^* = \frac{1}{\sqrt{q}} \text{ and } \omega_a^* = 1, \tag{5}$$

respectively.

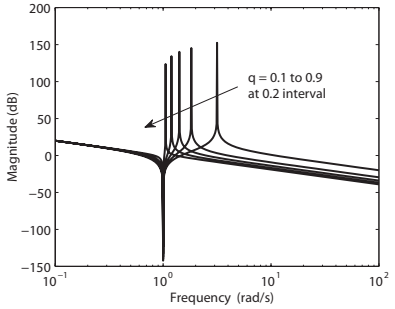

Fig. 2. Bode magnitude plots for the normalized two-mass model.

As shown in Fig. 2, with an increasing q the two resonance frequencies, ω_r^* and ω_a^* tend to become close, i.e., exhibiting the tendency of pole/zero cancellation. It is well known that the pole/zero cancellation leads to poor robustness of a closed-loop control system. In addition, the lower

the resonance frequency ω_r^*, the larger the required damping, which may lead to a smaller stability margin and/or a narrower bandwidth. For the controller design when q is large, it is essentially important to have a balanced tradeoff among damping, robustness and the speed of response.

3 Preliminary Discussion

In order to establish a baseline for dealing with more complex systems, ideal all-pole closed-loop systems are first discussed,

$$G(s) = \frac{a_0}{a_n s^n + a_{n-1}s^{n-1} + \ldots + a_1 s + a_0}. \quad (6)$$

Its characteristic polynomial $P(s)$ can be rewritten as

$$P(s) = \frac{1}{\gamma_{n-1}\gamma_{n-2}^2 \cdots \gamma_1^{n-1}}(\tau s)^n + \ldots + \frac{1}{\gamma_1}(\tau s)^2 + (\tau s) + 1, \quad (7)$$

where characteristic ratios γ_i (i=1,…,n-1) and generalized time constant τ are defined as

$$\gamma_1 = \frac{a_1^2}{a_0 a_2},\ \gamma_2 = \frac{a_2^2}{a_3 a_1}, \ldots, \gamma_{n-1} = \frac{a_{n-1}^2}{a_{n-2}a_n}, \quad (8)$$

$$\tau = \frac{a_1}{a_0}, \quad (9)$$

respectively. It can be seen that the time response of the all-pole closed-loop system is sped up by a factor of $1/\tau$, while all other time-domain specifications are solely determined by the characteristic ratios.

For the all-pole systems, overshoot is determined by the set of the characteristic ratios. $G(s)$ has monotonically decreasing magnitude in frequency response, and thus small overshoot under the condition that all the characteristic ratios are larger than two [1]. And the influence of each characteristic ratio on the overall performance can be evaluated by its system sensitivity

$$S_{\gamma_i}(s) = \frac{\partial G(s)/G(s)}{\partial \gamma_i/\gamma_i} \text{ for } i = 1, \ldots, n-1. \quad (10)$$

As illustrated in Fig. 3, the lower-index characteristic ratios have a more dominant influence because they affect more coefficients of the characteristic polynomial $P(s)$.

Considering 1) the characteristic ratio assignment of $\gamma_i > 2$ (i=1, …, n-1) as a starting point; 2) the dominant influence of low-index characteristic ratios, overshoot could be adjusted using a single characteristic ratio γ_1 (i.e., $\gamma_1 \geq 2$) while all higher-index characteristic ratios are fixed at two. Due to the difficulty in finding the exact analytical solutions

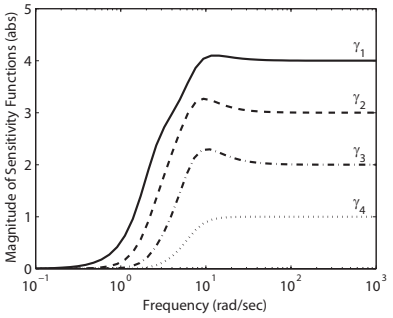

Fig. 3. Magnitude of the sensitivity functions $S_{\gamma_i}(s)$ for the fifth-order system (all the nominal values of γ_i are equal to two).

for systems of order higher than two, the minimum values of γ_1 for nonovershooting step responses are numerically determined and listed in Tab. 1. Then a nominal CRA can be defined as

$$\gamma_1 = \gamma_1^* \text{ and } \gamma_i = 2 \text{ for } i = 2, \ldots, n-1. \quad (11)$$

For the all-pole closed-loop systems, the overshoot and the speed of response can be independently specified [see Eqn. (7) and Fig. 4]. However, for a more general non-all-pole system such as the two-mass system, the effect of the pair of the jω-axis zeros impose additional limitations on the assignment of both the characteristic ratios and the generalized time constant.

Table 1. Minimum γ_1 for nonovershooting step responses.

System order	3	4	5	6	7	8
γ_1^*	2.61	2.53	2.48	2.48	2.48	2.48

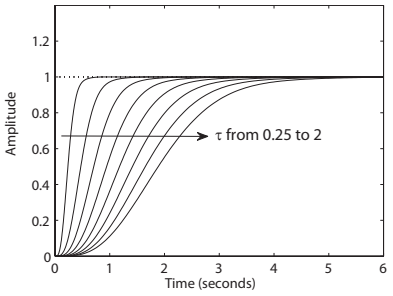

Fig. 4. Step responses of the fifth-order all-pole closed-loop system with a varying τ from 0.25 to 2 at 0.25 interval.

4 Low-order Controller Design

Two low-order control configurations, the IP and m-IPD controllers are adopted here for the velocity control of the two-mass system, as shown in Fig. 5. These special PID controllers are widely used in servo industry because the discontinuity of the reference command ω_{ref} can be smoothed by the integral controller. The low-pass filter $\frac{1}{T_d s+1}$ is necessary for implementing the derivative controller, and it is in a

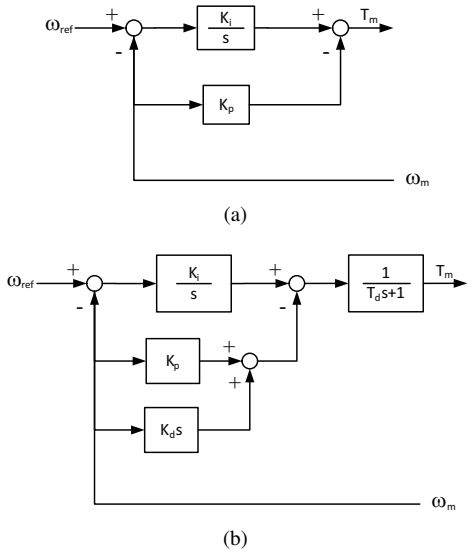

Fig. 5. Control configurations for the velocity control of the two-mass system. (a) IP controller. (b) m-IPD controller.

location that does not introduce any additional zero into the closed-loop transfer function. Considering the fundamental influence of poles, the nominal CRA in Eqn. (11) could also provide a good starting point for the controller design of the non-all-pole two-mass system, as illustrated in following sections.

4.1 IP Controller

The closed-loop transfer function for the IP feedback control loop is

$$G_n(s^*) = \frac{K_i^*(s^{*2}+1)}{qs^{*4}+K_p^*s^{*3}+(1+K_i^*)s^{*2}+K_p^*s^*+K_i^*}. \quad (12)$$

The characteristic ratios are

$$\gamma_1 = \frac{K_p^{*2}}{K_i^*(1+K_i^*)}, \quad (13)$$

$$\gamma_2 = \frac{(1+K_i^*)^2}{K_p^{*2}}, \quad (14)$$

$$\gamma_3 = \frac{K_p^{*2}}{q(1+K_i^*)}, \quad (15)$$

respectively. A controller design strategy could be to guarantee $\gamma_1 = \gamma_1^*$ and $\gamma_2 = 2$ for the fourth-order closed-loop system, while letting γ_3, the characteristic ratio with the highest index be jointly determined by q, K_p^* and K_i^*. K_i^*, K_p^* and thus the generalized time constant τ can then be calculated as

$$K_i^* = \frac{1}{2\gamma_1^*-1},\ K_p^* = \frac{1}{\sqrt{2}\left(1-\frac{1}{2\gamma_1^*}\right)},\ \tau = \frac{2\gamma_1^*}{\sqrt{2}}. \quad (16)$$

As shown in Fig. 6(a)(b), sufficient damping (i.e., nonovershooting) is provided when q is smaller than or equal to 0.31, because $\gamma_1 = \gamma_1^*$, $\gamma_2 = 2$ and $\gamma_3 \geq 2$, while the step responses become oscillatory at larger q's due to the decreasing γ_3. The identical τ under the IP controller design explains the same speed of the responses. The speed of step responses can be adjusted by letting the two higher-index characteristic ratios, γ_2 and γ_3 be determined by a variable τ, while keeping γ_1 equal to γ_1^*. The lower bound of τ for a positive K_i^* can then be found as

$$\tau > \sqrt{\gamma_1^*}. \quad (17)$$

However, deviations of γ_2 and γ_3 from their nominal value of two cause overshoot at a smaller generalized time constant.

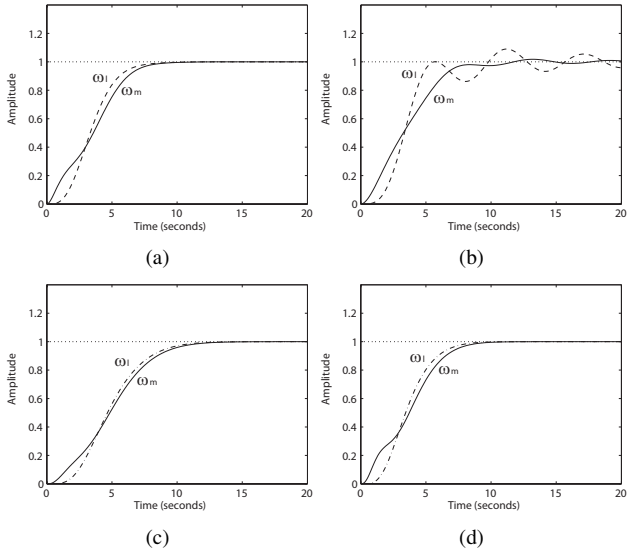

Fig. 6. Unity velocity step responses. (a) q=0.31 (IP control). (b) q=0.8 (IP control). (c) q=1/4 (m-IPD control). (b) q=0.8 (m-IPD control).

Meanwhile, the closed-loop transfer function of the IP control loop has two zeros $\pm j$. It is known that jω-axis zeros place a lower bound on the achievable settling time of a closed-loop system, i.e., the fastest speed of response that avoids an excessive overshoot [6]. The smooth step responses of the drive velocity ω_m in Fig. 6(a)(b) indicate that the determined generalized time constant τ is well above the lower bound imposed by the zeros of $\pm j$. However, the quantitative limitations imposed by the two jω-axis zeros are not yet fully understood and worthy of future research.

4.2 m-IPD Controller

The closed-loop transfer function of the m-IPD control can be derived as

$$G_n(s^*) = \frac{K_i^*(s^{*2}+1)}{a_5s^{*5}+a_4s^{*4}+a_3s^{*3}+a_2s^{*2}+a_1s^*+a_0}, \quad (18)$$

where

$$a_5 = qT_d^* = \frac{1}{\gamma_4\gamma_3^2\gamma_2^3\gamma_1^4}\tau^5 a_0 \tag{19}$$

$$a_4 = q + K_d^* = \frac{1}{\gamma_3\gamma_2^2\gamma_1^3}\tau^4 a_0 \tag{20}$$

$$a_3 = T_d^* + K_p^* = \frac{1}{\gamma_2\gamma_1^2}\tau^3 a_0 \tag{21}$$

$$a_2 = 1 + K_i^* + K_d^* = \frac{1}{\gamma_1}\tau^2 a_0 \tag{22}$$

$$a_1 = K_p^* = \tau a_0 \tag{23}$$

$$a_0 = K_i^*. \tag{24}$$

The following relationship can then be found as

$$\begin{bmatrix} a_0 \\ a_1 \\ a_2 - 1 \\ a_3 \\ a_4 - q \\ a_5 \end{bmatrix} = \begin{bmatrix} 0\ 1\ 0\ 0 \\ 1\ 0\ 0\ 0 \\ 0\ 1\ 1\ 0 \\ 1\ 0\ 0\ 1 \\ 0\ 0\ 1\ 0 \\ 0\ 0\ 0\ q \end{bmatrix} \cdot \begin{bmatrix} K_p^* \\ K_i^* \\ K_d^* \\ T_d^* \end{bmatrix}. \tag{25}$$

Eqn. (25) has a unique solution provided the ranks of both its coefficient matrix and augmented matrix are equal to four, i.e. the number of unknown controller parameters. Therefore, the coefficients of the characteristic polynomial must satisfy the following equations

$$a_2 - 1 - a_0 - (a_4 - q) = 0 \tag{26}$$

$$a_3 - a_1 - a_5/q = 0. \tag{27}$$

Equations (20)(22)(24)(26) yield

$$a_0 = \frac{1-q}{\frac{1}{\gamma_1}\tau^2 - \frac{1}{\gamma_3\gamma_2^2\gamma_1^3}\tau^4 - 1}. \tag{28}$$

In order to have a positive a_0, the upper and lower limits of τ ($\tau_{min} < \tau < \tau_{max}$) are

$$\tau_{max,\ min} = \gamma_1\gamma_2\sqrt{\frac{1 \pm \sqrt{1 - \frac{4}{\gamma_3\gamma_2^2\gamma_1}}}{2}\gamma_3} \tag{29}$$

respectively, whereas for a_5 to be positive, a_3 must be larger than a_1, i.e., the lower limit of τ is further restricted to

$$\tau_{min} = \sqrt{\gamma_2\gamma_1^2}. \tag{30}$$

Similarly, τ can be determined using Eqs. (19)(21)(23)(27)

$$\frac{1/q}{\gamma_4\gamma_3^2\gamma_2^3\gamma_1^4}(\tau^2)^2 - \frac{1}{\gamma_2\gamma_1^2}(\tau^2) + 1 = 0. \tag{31}$$

The value of τ cannot be independently specified if the nominal CRA for the fifth-order closed-loop system is to be guaranteed. For real and positive solutions of τ^2, it can be found that

$$q \geq \frac{1}{4}. \tag{32}$$

The smaller one in the two positive solutions of τ is within the limits defined in Eqs. (29)(30) for all the q's larger than one quarter. With the determined generalized time constant and the nominal CRA, the unique solution of the four m-IPD controller parameters can be simultaneously calculated instead of depending on the conventional trial-and-error-based techniques. The unity step velocity responses under the m-IPD control are shown in Fig. 6(c)(d).

Although m-IPD control under the nominal CRA provides sufficient damping, the controller design largely ignores the requirement on robustness because only the damping is emphasized [7]. As shown by the Bode plots of the loop transfer functions in Fig. 7, the m-IPD control provides a limited phase margin when q is large such as q=0.8. The infinity-norm of the complementary sensitivity function, $\| T(s) \|_\infty$, also shows a similar trend of the robustness with an increasing q [see Tab. 2]. In order to recover robustness performance, necessary sacrifices on damping and/or response speed are required. This can be achieved by allowing γ_4 to vary, which has the smallest overall influence. The generalized time constant τ can then be arbitrarily specified between τ_{min} and τ_{max}. As shown in Fig. 8, the poor robustness under the nominal CRA can be explained by the large positive K_d^*, i.e. the positive feedback of the D control signal. It is interesting to notice that with an increasing τ, damping is becoming to be mainly provided through a large T_d^* and the negative K_d^* eventually becomes positive. On the other hand, an excessively large τ leads to instability due to a negative coefficient a_0 in the characteristic polynomial. This classical tradeoff observed here well demonstrates the generality of the polynomial method, because its design procedure depends on the closed-loop characteristic polynomial instead of a specific control configuration.

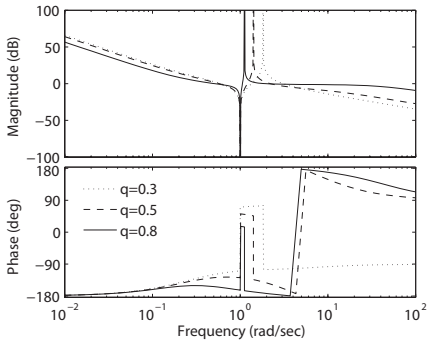

Fig. 7. The Bode plots of the m-IPD control's loop transfer functions under nominal CRA.

Table 2. Infinity-norms of complementary sensitivity function.

q	0.3	0.4	0.5	0.6	0.7	0.8
$\| T(s) \|_\infty$	1.22	1.35	1.54	2.42	4.34	8.33

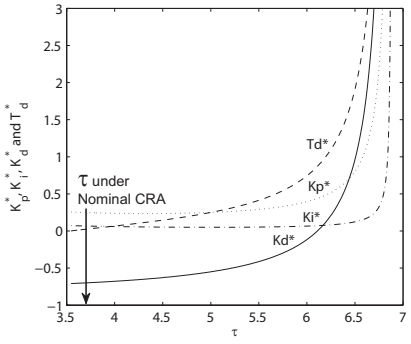

Fig. 8. m-IPD controller parameters versus generalized time constant τ ($q = 0.8$).

5 Experimental Results

By the different combination of the numbers of the flywheels at the drive and load sides, the inertia ratio q that the laboratory torsion system is capable of emulating ranges from 0.29 to 0.80. A thin shaft (4mm diameter with K_s=2.1204Nm/rad) is chosen, which enables the low resonance and anti-resonance frequencies of the two-mass system. The actual dynamics is obviously much more complicated than the dynamics described by the ideal two-mass model, especially with the existence of gear backlash [see Fig. 1]. This modeling error can be used to verify the robustness of the low-order controller design against nonlinearity.

The experimental velocity responses are shown in Figs. 9-12, in which a large load disturbance torque 2.5N·M is applied at 1.0 sec except in Fig. 10. The experimental results (black) well match the simulation results (red) except in Fig. 11(b) due to the gear backlash nonlinearity. This observation validates the above theoretical analysis and controller design. The IP control becomes ineffective at a large q such as 0.80 because γ_3 decreases greatly from its nominal value of two [see Fig. 9]. Its speed of response can be adjusted by specifying the generalized time constant τ; however, only γ_1 can be exactly assigned as its nominal value. The oscillatory responses in Fig. 10, when τ is small, can be explained by $\gamma_2 < 2$. The m-IPD control under nominal CRA is effective when q is small (such as 0.29 in Fig. 11(a)); however, at large q's the necessity of taking negative derivative gain causes poor robustness against gear backlash and disturbance torque as shown in Fig. 11(b). The m-IPD control's robustness performance can be improved by having a smaller γ_4 and thus a larger τ, i.e., less damping and slower speed of response [see Fig. 12].

6 Conclusions

The application of the polynomial method in the transient response control of a benchmark two-mass system is discussed in this paper. Two practical low-order control configurations, the IP and m-IPD controllers are designed. Unlike the ideal all-pole systems, additional limits arise due to the pair of the $j\omega$-axis zeros of the two-mass system and the specific control configurations. It is found that the characteristic ratios and the generalized time constant cannot be independently specified. And the jω-axis zeros and stability requirement place bounds on the achievable generalized time constant. The demonstrated relationship between the transient responses and the assignments of the characteristic ratios and the generalized time constant explains the effectiveness of the polynomial-method-based controller design, i.e. its capability of directly addressing time-domain specifications such as overshoot and the speed of response during controller design.

The future works may include applying the polynomial method in the controller design of more complicated and realistic systems, such as robots and other industrial applica-

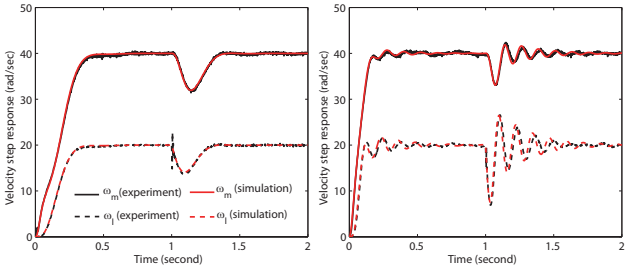

Fig. 9. Velocity step responses under IP control with γ_1=2.53 and γ_2=2. (a) q=0.29. (b) q=0.80.

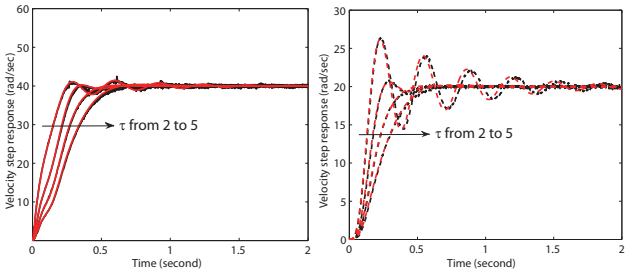

Fig. 10. Velocity step responses under IP control with q=0.29, γ_1=2.53 and τ from 2 to 5 at 1.0 interval. (a) Drive velocities. (b) Load velocities.

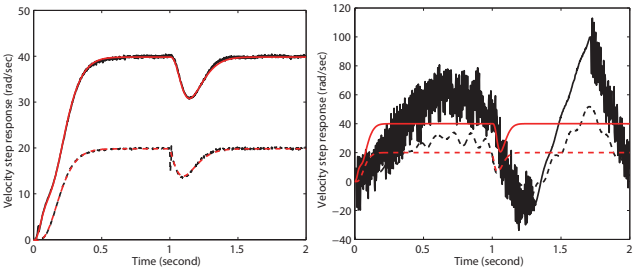

Fig. 11. Velocity step responses under m-IPD control with nominal CRA. (a) q=0.29. (b) q=0.80.

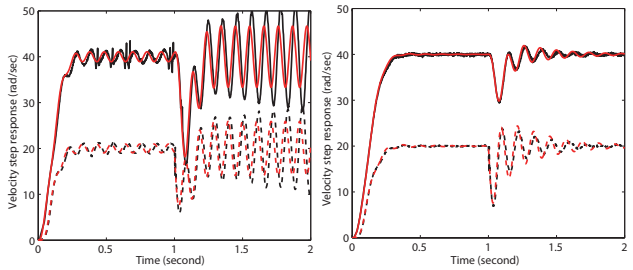

(a) (b)

Fig. 12. Velocity step responses under m-IPD control with γ_1=2.48, γ_2=2, γ_3=2 and specified τ's at q=0.80. (a) τ=5.5. (b) τ=6.5.

tions. It is also of practical importance to investigate a general design scheme for the control of higher-order systems such as a three-mass system, in which direct equation solving may either be infeasible or too complicated. In addition, extending the polynomial method to the design of multi-input-multi-output (MIMO) control systems would broaden its applications.

Acknowledgements

The authors would like to thank National Science Foundation of China, for supporting this work [grant number 50905113 (2010-2012)].

References

[1] Kim, Y. C., Keel L. H., and S. P. Bhattacharyya, 2003. "Transient Response Control via Characteristic Ratio Assignment", IEEE Trans. Automatic Control, **48**(12), pp. 2238-2244.

[2] Kim Y. C., Keel L. H., and Manabe S., 2002. "Controller Design For Time Domain Specifications", in Proceedings of the 15th IFAC Triennial World Congress, Barcelona, Spain.

[3] Naslin P., 1969. "*Essentials of Optimal Control*", Boston Technical Publishers Inc., Cambridge, MA.

[4] S. Manabe, 2003. "Importance of Coefficient Diagram in Polynomial Method", in Proceedings of the 42nd IEEE Conference on Decision and Control, Maui, Hawaii USA, pp. 3489-3494.

[5] Lee K. and Blaabjerg F., 2007. "An Improvement of Speed Control Performances of a Two-mass System Using a Universal Approximator", Electr Eng, **89**, pp. 389-396.

[6] Goodwin G. C., Woodyatt A. R., Middleton R. H. and Shim J., 1999. "Fundamental limitations due to $j\omega$-axis zeros in SISO systems", Automatica, **35**, pp. 857-863.

[7] Ma C., Cao J. and Qiao Y., 2013. "Polynomial Method Based Design of Low Order Controllers for Two-Mass System", IEEE Trans. Industrial Electronics, **60**(3), pp. 969-978.